20-nm-sized mesoporous silica nanoparticles with porphyrin photosensitizers for in vitro photodynamic therapy

Chiara Mauriello Jimenez[a], Yolanda Galàn Rubio[a], Valentin Saunier[a], David Warther[a], Vanja Stojanovic[b], Laurence Raehm[a], Céline Frochot[d], Philippe Arnoux[d], Marcel Garcia[b], Alain Morère[b], Nadir Bettache[b], Marie Maynadier[e], Philippe Maillard[c], Magali Gary-Bobo[b] and Jean-Olivier Durand[a]

[a] *Institut Charles Gerhardt Montpellier, UMR 5253, CC 1701 Equipe Ingénierie Moléculaire et Nano-objets, Place Eugène Bataillon, 34095 Montpellier Cedex 05, France*

[b] *Institut de Biomolécules Max Mousseron, UMR 5247, Avenue Charles Flahault, 34093 Montpellier Cedex 05, France*

[c] *Institut Curie-Recherche, UMR 176, Centre Universitaire, 91405 Orsay, France*

[d] *Laboratoire Réactions et Génie de Procédés, UMR 7274, 1 Rue Grandville, 54001 Nancy, France*

[e] *NanoMedSyn, 15 Avenue Charles Flahault, 34093 Montpellier Cedex 05, France*

Corresponding Author:

Chiara Mauriello Jimenez, chiaramauriellojimenez@gmail.com

Jean-Olivier Durand, durand@um2.fr

Abstract

We report the synthesis of 20-nm-sized mesoporous silica nanoparticles encapsulating three different porphyrin photosensitizers (PS). Synthesized by the sol–gel method, in the presence of cetyltrimethylammonium bromide surfactant and tetraorthosilicate as silica source, we developed those nanoparticles with the aim of treating cancer cells using photodynamic therapy. The colloidal stability, due to the PEG-silane chain grafted on the surface, was demonstrated at 37 ——————————C in cell culture medium. Then, nanoparticles were functionalized by silylated squarate mannose and used in MCF-7 breast cancer cells for one-photon therapy. Promising results were obtained after 5 h of incubation.

Keywords

Porphyrin, Mesoporous, Silica nanoparticles, Functionalization, PDT

Graphical abstract

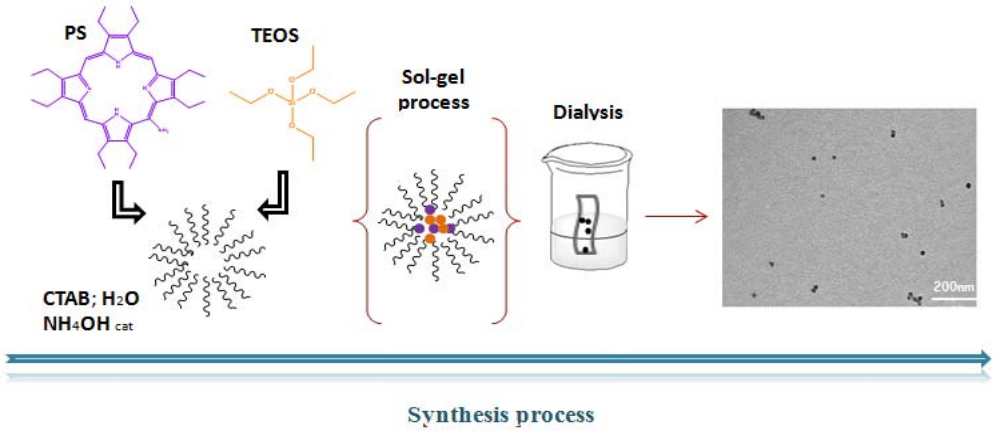

Introduction

Mesoporous Silica Nanoparticles have attracted much attention in different fields in the last decade and particularly for biological applications. The field has been extensively reviewed. [1-29] Indeed their tunable pore size, flexible functionalization, and high specific surface area [30,31] allowed the use of MSN in many different applications such as antireflective coatings [32], catalysis, [33] sensors [34] and biology. [35] The usual size of MSN obtained from classical synthetic methods leads to diameters of about 100 nm. However the size reduction of MSN with diameters below 50 nm has been the subject of much effort over the last 6 years. Indeed small-sized MSN are particularly attractive for applications in material science [36] or biology, [37] and the mechanism of their synthesis has been recently investigated. [38] The pioneering works in down-sizing MSN diameter were performed by the groups of Kuroda, Huo, Mou, in 2009 [39-41] and by the group of Wiesner who reached diameter below 10 nm. [42,43] Small-sized MSN were used by Shi and co-workers [44,45] and others [46] for cancer applications. These nanoparticles conjugated with TAT peptide were able to target the nuclei of cells in vitro and in vivo and very efficient photodynamic therapy application [47] was described. In the course of our work on photodynamic therapy with silica-based particles, [48,49] we were interested in small-sized MSN in order to cross-biological membranes. We performed the synthesis of mannose-functionalized 20 nm diameter MSN but as the outer specific surface area increased, the colloidal stability of the particles was difficult to achieve.[50] Finally we managed to image retinoblastoma cells. In the continuation of this work, we present here the syntheses and characterizations of mannose-functionalized small-sized MSN possessing porphyrin photosensitizers in the walls of the MSN towards photodynamic therapy applications.

Experimental

2.1 Materials and general procedures

ACS reagents grade starting materials and solvents were used as received without further purification.
Ammonium 4,4',4''-(20-(4-aminophenyl) porphyrin-5,10,15-triyl)tribenzenesulfonate (**POR a**) and 3-(2,5-dioxo-2,5-dihydro-1H-pyrrol-1-yl)-N-(3-(4-(10,15,20-tri(pyridin-4-yl)porphyrin-5-yl) phenoxy) propyl) propanamide (**POR b**) were synthesized as described [51,49].
5-(amino)-2, 3, 7, 8, 12, 13, 17, 18-(octaethyl) porphyrin was purchased from Pophychem (**POR c**).
3-((4-(((2R, 3S, 4S, 5S, 6R)-3, 4, 5-trihydroxy-6-(hydroxymethyl) tetrahydro-2H-pyran-2-yl) oxy) phenyl) amino)-4-((3-(trimethoxysilyl) propyl) amino) cyclobutane-1, 2-dione (*silylated squarate mannose, Mannose-Si)*) was obtained from a reported procedure by D.Warther et al. (RSC Adv. **2014**, 4, 37171-37179).
Cetyltrimethylammonium bromide (CTAB) was purchased from Alfa Aesar, tetraethyl orthosilicate (TEOS), amino-propyltriethoxy silane (APTS), isocyanatopropyltriethoxy silane (IPTS), (3-mercapto propyl)trimethoxysilane (MPS) and ammonium hydroxide were purchased from Sigma-Aldrich. (6-[2-(2-[2-Methoxy-ethoxy]-ethoxy)-ethoxy] hexyl) trimethoxysilane (PEG-Si) and 11-amino-undecyltrimethoxysilane (NH_2-Si) were purchased from SiKEMIA. Ultrapure water was obtained with a Barnstead™Easypure™RoDi from Thermo Scientific. DLS measurements were performed on a Vasco Particle Size Analyzer DL135 from Cordouan Technologies and analyzed with nanoQ software. ^{1}HNMRspectra was recorded on a Bruker AC-300 spectrometer. Chemical shifts (in δ units, ppm) are referenced to TMS using DMSO-d_6 (δ = 2.50 ppm) as the internal standard. IR spectra spectra were recorded on a Perkin-Elmer 100 FT spectrophotometer. UV-visible spectra were obtained using a Perkin-Elmer spectrometer (molar extinction coefficient value is given in L $mol^{-1}cm^{-1}$). TEM images were taken on a JEOL 1200 EXII, 120 kV.

2.2 Preparation of POR1 - POR2 - POR3 (Scheme 1)

PORa [49] and **PORb** [51] precursors were silylated overnight at room temperature following the procedure already described. **PORc** was silylated with isocyanatopropyltriethoxysilane. Briefly: 3.1 mg (5.45 µmol) of the photosensitizer were dissolved in 1 mL of tetrahydrofurane, 4.2 µL (3 eq.) of isocyanatopropyltriethoxysilane and 4.4 µL (5 eq.) of diisoproylethylamine were added. The reaction was stirred at room temperature for 12 h.
^{1}H NMR POR3 (300 MHz, DMSO): δ 7.31(s, 1H, pyrr-CH-pyrr), 7.09(s, 1H, pyrr-CH-pyrr), 6.05(s, 1H, pyrr-CH-pyrr), 5.75(s, 1H, CO-NH-CH_2), 4.36(s, 1H, CO-NH-porh), 3.75 (q, ^3J = 6.8 Hz, 6H, O-CH_2-CH_3), 3.60 (t, ^3J = 6.0 Hz, 16H, CH_3-CH_2-porph), 1.76 (t, ^3J = 6.4 Hz, 24H, CH_3-CH_2-porph), 1.66 – 1.54 (m, 4H, CH_2-CH_2-CH_2-Si), 1.15 (t, ^3J = 7.0 Hz, 9H, O-CH_2-CH_3), 0.66 – 0.54 (t, ^3J = 7.0 Hz, 2H, CH_2-Si).

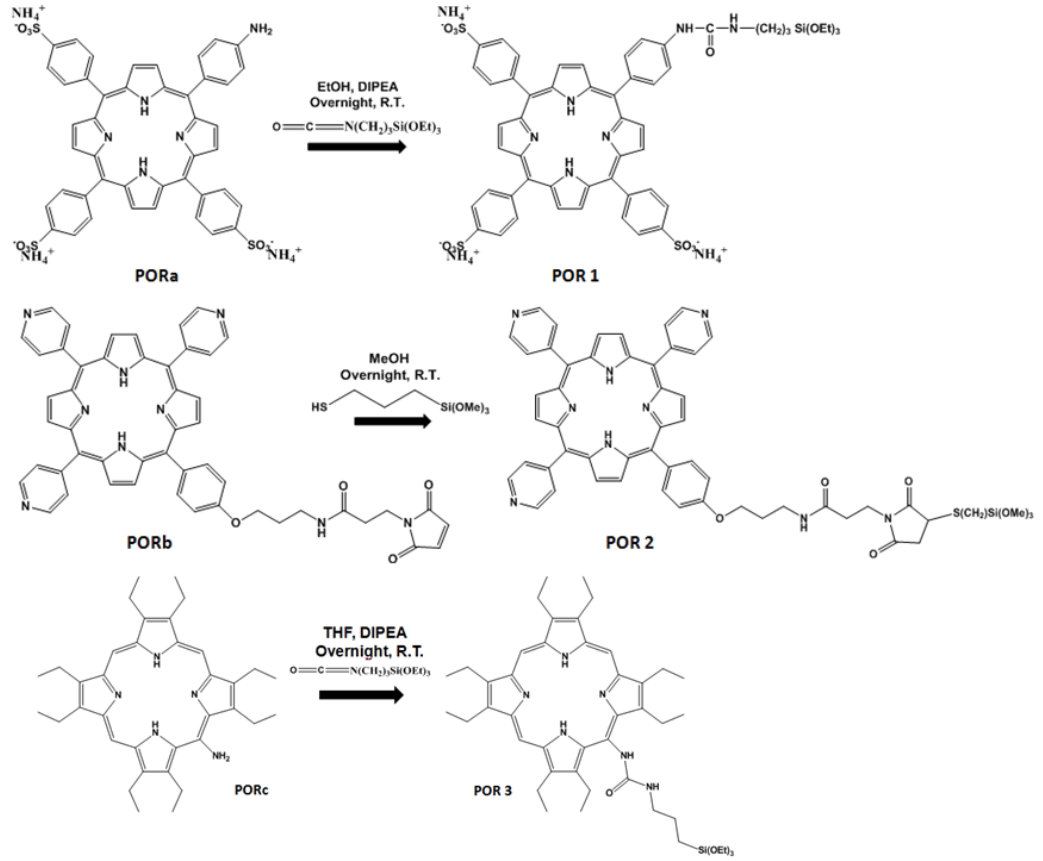

Scheme 1 Silylation of the POR precursors.

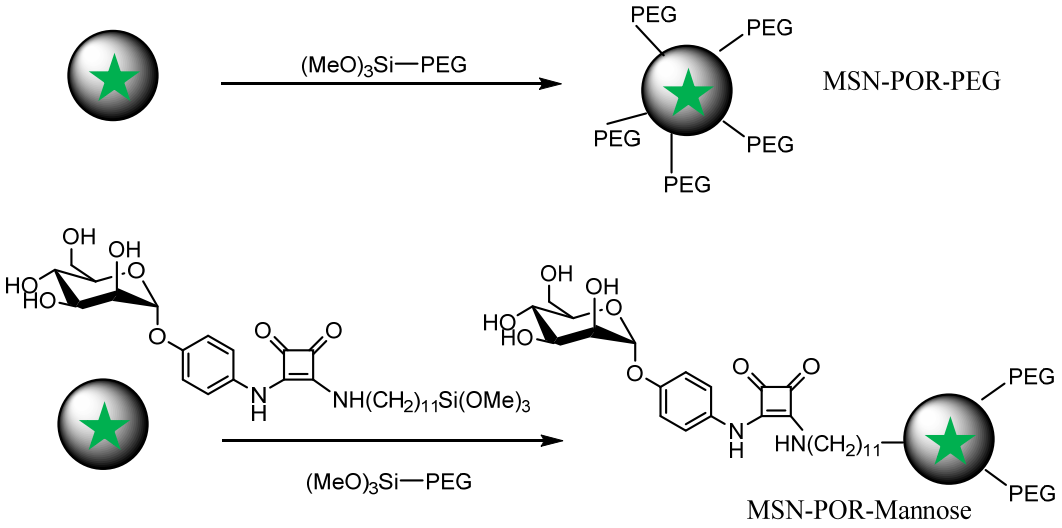

Scheme 2 Surface functionalization of MSN following ref [50].

2.3 Synthesis of 20 nm sized mesoporous silica nanoparticles: Intermediary solution (I)

A mixture of 816 mg of CTAB (2.24 mmol; 0.5 eq.), ultrapure water(100 mL) and 1 mL of a freshly prepared solution of NH4OH 0.2 M (0.2 mmol; 0.04 eq.) was stirred at 50°C for 2 hours at 500 rpm in a 250 mL three neck round bottom flask. Then, the photosensitizer POR (0.3mL, $1.63*10^{-3}$mmol) was added to the aforementioned solution. After 30 seconds, tetraorthosilicate (1mL) was fastly added to the mixture and the condensation process was conducted overnight. Afterwards, the solution was cooled at room temperature and stored without purification.

2.4 Surface stabilization : PEG-Si chain (MSN-POR-PEG) (Scheme 2)

10 mL of the solution aforementioned (*solution I*) was stirred at 50°C at 500 rpm in a Schlenck. Then, 126 mg of PEG-Si was added and the mixture was stirred overnight at the same temperature. Once the solution was cooled, purification and extraction of the surfactant was done by dialysis process (cut off 12 kDa) in a mixture of EtOH/H_2O/AcOH: 1/1/0.07 for 24 hours. The operation was renewed 2 times. The suspension was then dialyzed in EtOH for 3 times for 24 hours and stored at room temperature in EtOH.

2.5 Surface stabilization and functionalization by *Mannose-Si* (MSN-POR-Mannose)

MSN-POR-Mannose were functionalized on the surface as described [50]. Briefly, 10 mL of the solution aforementioned (*solution I*) was stirred at 50°C at 500 rpm in a Schlenck. Then, 126 mg of PEG-Si was added along with a solution of Mannose-Si in DMSO (13 mg in 0.4 mL of DMSO) and the mixture was stirred overnight at the same temperature. Extraction and purification process was done as mentioned before.

2.6 Determination of singlet oxygen quantum yield [ϕ ($^1O_2$)]

Excitation occurred with a Xe-arc, the light was separated in a SPEX 1680, 0.22µm double monochromator. The detection at 1270 nm was done through a PTI S/N 1565 monochromator, and the emission was monitored by a liquid nitrogen-cooled Ge-detector model (EO-817L, North Coast Scientific Co). The absorbance of the reference solution (Rose Bengal in EtOH ϕ ($^1O_2$) = 0.681 and the sample solution (at 422 nm) were set equal (between 0.2 and 0.5) by dilution.

2.5. In vitro one-photon photodynamic therapy (PDT) experimental settings

MCF-7 human breast cancer cells were cultured in Dulbecco's modified Eagle'smedium (DMEM) supplemented with 10% fetal bovine serum and 50 µg.mL-1 gentamycin. All cells were allowed to grow in humidified atmosphere at 37°C under 5% CO2. For *in vitro* phototoxicity, MCF-7 cells were seeded into a 384 multiwell glass-bottomed plate (thickness 0.17 mm), with a black polystyrene frame, 2000 cells per well in 50 µL of culture medium, and allowed to grow for 24 h. NPs were then dispersed under ultrasounds in PBS at a concentration of 1 mg.mL-1 and cells were then incubated for 5 h with or without nanoparticles at a final concentration of 80 µg.mL-1 in supplemented DMEM. After incubation with NPs, cells were washed twice, maintained in fresh culture medium, and then submitted (or not) to laser irradiation. After 2 days, the MTS assay was performed and was corrected.

3. Results and discussion

3.1 Syntheses of mesoporous silica nanoparticles of 20 nm diameter

Firstly, nanoparticles were synthesized by the sol-gel procedure at 50°C overnight in the presence of TEOS and silylated porphyrins POR 1-3 (*solution I*). Then, 10 mL of the solution were stirred overnight with PEG-Si at 50°C and then were dialyzed for 6 days in order to remove the surfactant. MSN-POR-PEG were obtained. DLS analysis confirmed the non aggregation of the nanoparticles. DLS and TEM of MSN-POR1-PEG are depicted in figure 1a. PEG-Si allowed stabilizing the nanoparticles. We obtained monodisperse solution of nanoparticles with a hydrodynamic diameter of 20 nm. TEM image showed nanoparticles of 18 nm which was in agreement with DLS measurements (Fig. 1d). The same results were obtained with POR 2 (Fig. 1b; 1e) and POR3 (Fig. 1c; 1f)

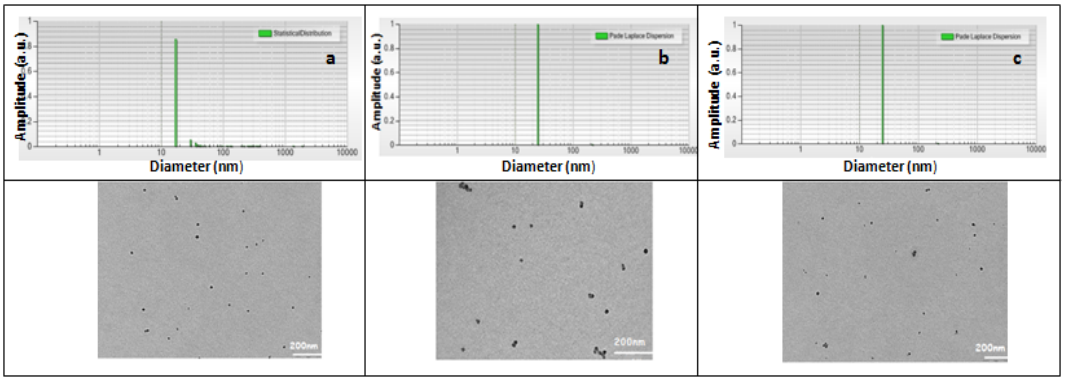

Fig1. a-c) DLS of MSN-POR1-PEG, MSN-POR2-PEG and MSN-POR3-PEG after dialysis. d-f) TEM images of the corresponding MSN-POR-PEG nanoparticles. Images showed an homogenous size of nanoparticles (scale bar: 200 nm).

The MSN were also functionalized with PEG and mannose following a procedure recently described. The MSN-POR2-Mannose were analyzed by Dynamic Light Scattering (DLS) at 37 º C, to study their stability at physiologic temperature (Fig. 2). On top, nanoparticles were firstly tested in saline conditions with PBS at 25 ºC and then at 37ºC for 40 min. Therefore 1 mL containing 10 mg/mL of MSN-POR2-Manniose were added to 1 mL of PBS and the suspension was homogenized by sonication and allowed to stay for 24 hours at room temperature.
On the bottom, their stability was studied in a mixture of cell culture medium (GIBCO) with 20% fetal bovine serum, 100 U mL^{-1} of penicillin and 100 gmL^{-1} of streptomycin. According to that, 500 µL of the nanoparticles solution were diluted in 500 µL of the cell culture medium and treated as mentioned before. As it can be observed, the size distribution is similar at 25ºC and 37ºC and the prepared MSN were stable in the cell culture medium.

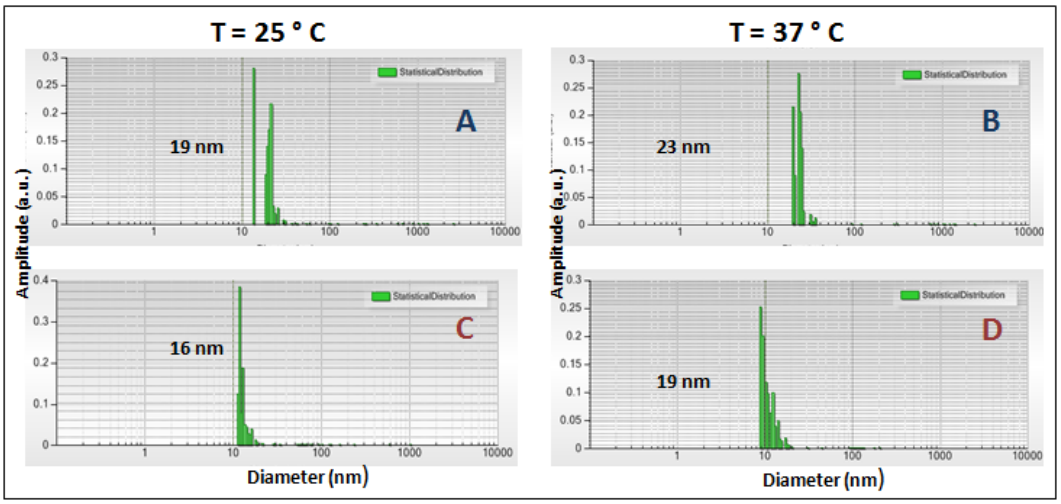

Fig.2. DLS of MSN-POR2-PEG-Mannose. a-b) Measurements in PBS at 25°C and 37°C.c-d) Measurements in cell culture medium at 25°C and 37°C.

The specific surface area and pore characteristics of MSN-POR2 after dialysis were examined using the nitrogen adsorption desorption measurements. As shown in Fig.3a, NPs present typical IV isotherm characteristics with defined step at a relative pressure of 0.4. It can be observed an hysteresis at 0.8 corresponding to the interparticle aggregates. This phenomenon is confirmed by BJH analysis of pore size (Fig. 3b). The first band at 2.5 nm corresponds to the pore size and the second and third band at 5 nm and 9.6 nm respectively, corresponds to the space between nanoparticles. The specific surface area was 840 m^2/g and the pore volume was 1.28 cm^3/g.

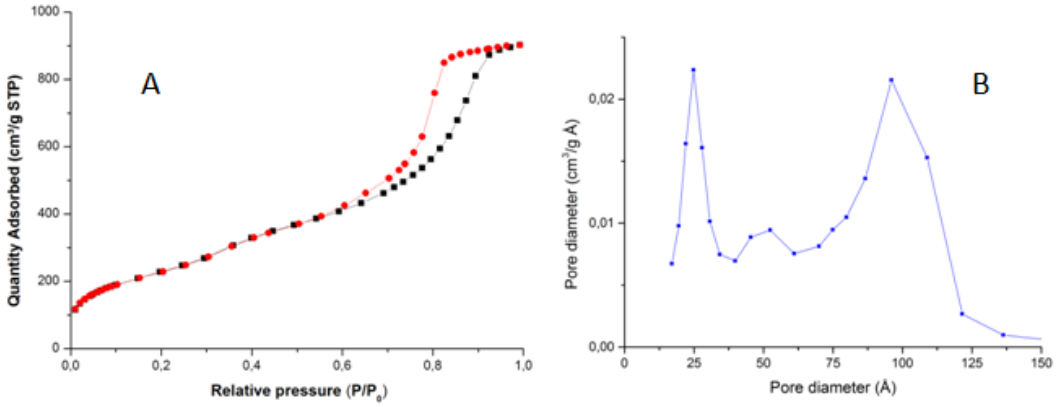

Fig.3. a) The N_2 adsorption-desorption isotherms and b) the pore distribution of NPs.

The amount of photosensitizer and the targeting biomolecule was determined by quantitative analysis of the intensity of the absorption spectra bands. The UV-Visible absorption spectra of 1 ml of MSNs solutions (1mL in EtOH contains 10 mg of MSN) and POR are shown in Fig. 4. The quantity of porphyrin was determined using the Soret band at 420 nm and the quantity of Mannose was determined at 340 nm, using the beer Lambert law (Table 1). The first spectra group of the anionic porphyrin (POR 1), MSN-POR1-PEG and MSN POR1-Mannose are presented in figure 4A. We observed that the soret and Q bands of POR1 are not shifted after encapsulation in agreement with well dispersed and non-aggregated POR1 in MSN. UV-Vis spectra of POR2, MSN-POR2-PEG, MSN-POR2-Mannose are presented in fig 4B. Comparing the spectra of MSN-POR2 with POR2, a modification of the Q bands was observed. This is probably due to the formation of aggregates of POR2 inside the nanoparticles. The concentration of POR2 in MSN is indeed three times more important than POR1. In Figure 4C, UV-Vis spectra of POR 3 and the corresponding MSNs are depicted. At 420 nm, a red shift of the Soret band was observed and it can be also observed that the four Q bands of POR3 are changed in two Q bands when POR3 was encapsulated in MSN. The disparition of two Q bands is due to the formation of the dication of the porphyrin by the treatment with AcOH during the dialysis process (Fig. 4D). With the addition of acid, the symmetry of porphyrin is changed from a D2h wich is corresponding to a free-base porphyrin, to a D4h symmetry wich is corresponding to the attachment of protons to the two imino nitrogens of the pyrrole rings of the porphyrin.

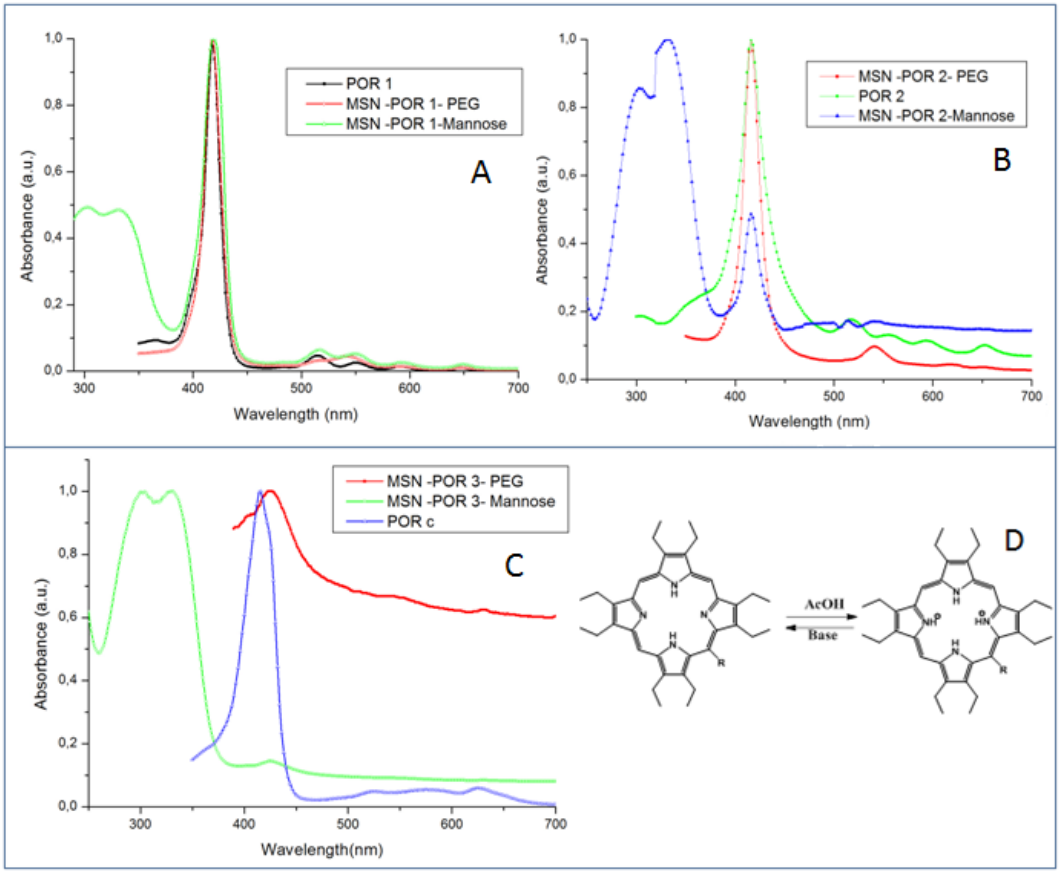

Fig. 4.a-b-c) UV spectra in EtOH of the different porphyrins and their materials and d) schema of protonation of the free base porphyrin c under acidic conditions.

	Porph. [c] (µmol/g NPs)	**Mannose [c] (µmol/g NPs)**
MSN-POR 1-Mannose	1	14
MSN-POR 2-Mannose	3	11
MSN-POR 3-Mannose	0.1	5

Table 1. Quantification of porphyrin and mannose in NPs.

The quantum yield of singlet oxygen production obtained by $^1O_2$ phosphorescence measurements in EtOH, with Rose Bengal used as standard reference, was calculated to be 43% for MSN-POR1-Mannose and 47% for MSN-POR2-Mannose (Fig. 5). Therefore, MSN-POR2-Mannose were subsequently used for PDT of MCF-7 breast cancer cells.

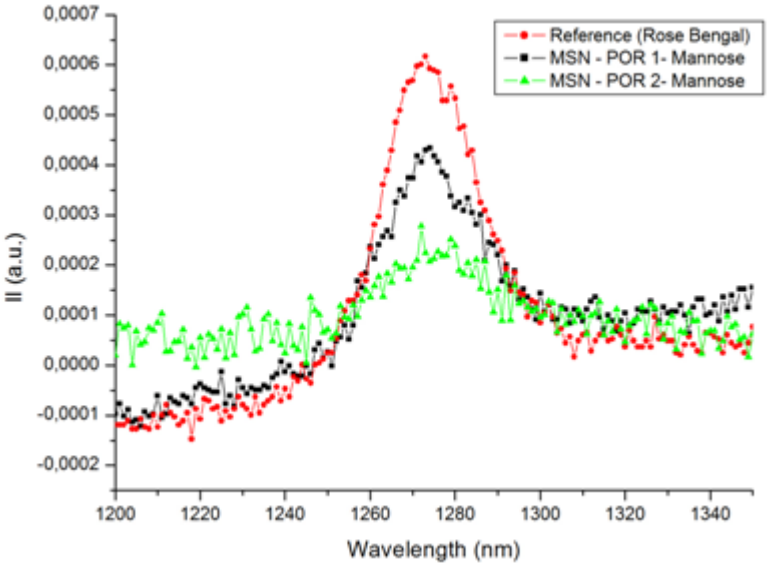

Fig.5. Determination of MSN-POR1-Mannose and MSN-POR2-mannose singlet oxygen quantum yields (λ ex = 422 nm) using Rose Bengal as reference in EtOH.

3.2 Phototoxicity

Breast cancer cells (MCF-7) were incubated with the photo-activable MSN-POR2-Mannose at 80µg mL^{-1} for 5 h at 37°C and irradiated for 10 min (λ= 420 nm) or not. The MTT assay was the performed after two days to assess the citotoxicity of the nanoparticles (Fig. 6). The nanoparticles were not cytotoxic at 80µg mL^{-1} in the dark. After irradiation, MSN-POR2-Mannose showed photocytotoxicity wich is in agreement with $^1O_2$ formation. Cell death was observed after 3 hours of incubation wich confirmed a rapid cellular uptake of the MSN.

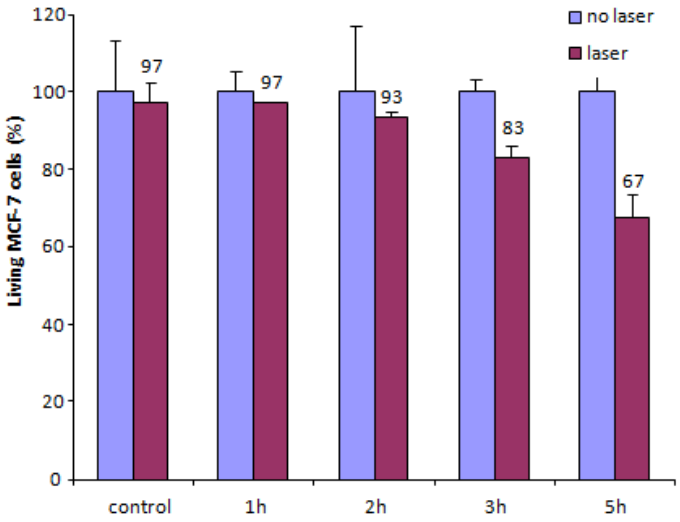

Fig.6. PDT of MSN-POR2-Mannose (irradiated at 420 nm) on breast cancer cells. MSN concentration of 80 µg mL^{-1}.

Conclusion

20 nm mesoporous silica nanoparticles covalently encapsulating porphyrin photosensitizers have been successfully prepared by the sol gel procedure in presence of CTAB and TEOS. The surface of the nanoparticles was functionalized with PEG or PEG and mannose. The stability of the prepared nanoparticles was demonstrated by DLS analyses at 25°C and 37°C in PBS and in culture medium.

MSN-POR1-Mannose and MSN-POR2-Mannose were able to produce singlet oxygen and preliminary PDT experiments with MSN-POR2-Mannose were successfully performed on breast cancer cells.

Ackowledgments

Support from the Agence Nationale de la Recherche ANR nanoptPDT and the FEDER

Languedoc-Rousssillon project N°41470 are gratefully acknowledged. Laure Lichon of

IBMM is thanked for her technical assistance.

References

1. Knezevic NZ, Durand J-O (2015) Large pore mesoporous silica nanomaterials for application in delivery of biomolecules. Nanoscale 7 (6):2199-2209. doi:10.1039/c4nr06114d
2. Knezevic NZ, Durand J-O (2015) Targeted Treatment of Cancer with Nanotherapeutics Based on Mesoporous Silica Nanoparticles. ChemPlusChem 80 (1):26-36. doi:10.1002/cplu.201402369
3. Zhang Y, Yan J, Liu S (2014) Biocompatibility and biomedical applications of functionalized mesoporous silica nanoparticles. Biointerface Res Appl Chem 4 (3):767-775, 769
4. Yang K-N, Zhang C-Q, Wang W, Wang PC, Zhou J-P, Liang X-J (2014) pH-responsive mesoporous silica nanoparticles employed in controlled drug delivery systems for cancer treatment. Cancer Biol Med 11 (1):34-43
5. Nadrah P, Planinsek O, Gaberscek M (2014) Stimulus-responsive mesoporous silica particles. J Mater Sci 49 (2):481-495
6. He Q, Shi J (2014) MSN Anti-Cancer Nanomedicines: Chemotherapy Enhancement, Overcoming of Drug Resistance, and Metastasis Inhibition. Adv Mater 26 (3):391-411
7. Dave PN, Chopda LV (2014) A review on application of multifunctional mesoporous nanoparticles in controlled release of drug delivery. Mater Sci Forum 781 (Multi-Functional Nanomaterials and Their Emerging Applications):17-24, 19 pp
8. Argyo C, Weiss V, Braeuchle C, Bein T (2014) Multifunctional Mesoporous Silica Nanoparticles as a Universal Platform for Drug Delivery. Chem Mater 26 (1):435-451
9. Mai WX, Meng H (2013) Mesoporous silica nanoparticles: A multifunctional nano therapeutic system. Integr Biol 5 (1):19-28. doi:10.1039/c2ib20137b
10. Mody KT, Popat A, Mahony D, Cavallaro AS, Yu C, Mitter N (2013) Mesoporous silica nanoparticles as antigen carriers and adjuvants for vaccine delivery. Nanoscale 5 (12):5167-5179
11. Mamaeva V, Sahlgren C, Linden M (2013) Mesoporous silica nanoparticles in medicine-Recent advances. Adv Drug Deliv Rev 65 (5):689-702. doi:10.1016/j.addr.2012.07.018
12. Duan R, Xia F, Jiang L (2013) Constructing Tunable Nanopores and Their Application in Drug Delivery. ACS Nano 7 (10):8344-8349
13. Douroumis D, Onyesom I, Maniruzzaman M, Mitchell J (2013) Mesoporous silica nanoparticles in nanotechnology. Crit Rev Biotechnol 33 (3):229-245
14. Chen Y, Chen H, Shi J (2013) In Vivo Bio-Safety Evaluations and Diagnostic/Therapeutic Applications of Chemically Designed Mesoporous Silica Nanoparticles. Adv Mater 25 (23):3144-3176. doi:10.1002/adma.201205292
15. Yang P, Gai S, Lin J (2012) Functionalized mesoporous silica materials for controlled drug delivery. Chem Soc Rev 41 (9):3679-3698. doi:10.1039/c2cs15308d
16. Vivero-Escoto JL, Huxford-Phillips RC, Lin WB (2012) Silica-based nanoprobes for biomedical imaging and theranostic applications. Chem Soc Rev 41 (7):2673-2685. doi:10.1039/c2cs15229k
17. Tang F, Li L, Chen D (2012) Mesoporous Silica Nanoparticles: Synthesis, Biocompatibility and Drug Delivery. Adv Mater 24 (12):1504-1534. doi:10.1002/adma.201104763
18. Lin Y-S, Hurley KR, Haynes CL (2012) Critical Considerations in the Biomedical Use of Mesoporous Silica Nanoparticles. J Phys Chem Lett 3 (3):364-374
19. Li Z, Barnes JC, Bosoy A, Stoddart JF, Zink JI (2012) Mesoporous silica nanoparticles in biomedical applications. Chem Soc Rev 41 (7):2590-2605. doi:10.1039/c1cs15246g
20. Asefa T, Tao Z (2012) Biocompatibility of Mesoporous Silica Nanoparticles. Chem Res Toxicol 25 (11):2265-2284. doi:10.1021/tx300166u
21. Yang Y-W (2011) Towards biocompatible nanovalves based on mesoporous silica nanoparticles. Medchemcomm 2 (11):1033-1049. doi:10.1039/c1md00158b

22. Popat A, Hartono SB, Stahr F, Liu J, Qiao SZ, Lu GQ (2011) Mesoporous silica nanoparticles for bioadsorption, enzyme immobilisation, and delivery carriers. Nanoscale 3 (7):2801-2818. doi:10.1039/c1nr10224a
23. He Q, Shi J (2011) Mesoporous silica nanoparticle based nano drug delivery systems: synthesis, controlled drug release and delivery, pharmacokinetics and biocompatibility. J Mater Chem 21 (16):5845-5855
24. Vivero-Escoto JL, Slowing II, Trewyn BG, Lin VSY (2010) Mesoporous Silica Nanoparticles for Intracellular Controlled Drug Delivery. Small 6 (18):1952-1967
25. Coti KK, Belowich ME, Liong M, Ambrogio MW, Lau YA, Khatib HA, Zink JI, Khashab NM, Stoddart JF (2009) Mechanised nanoparticles for drug delivery. Nanoscale 1 (1):16-39
26. Slowing II, Vivero-Escoto JL, Wu C-W, Lin VSY (2008) Mesoporous silica nanoparticles as controlled release drug delivery and gene transfection carriers. Adv Drug Deliv Rev 60 (11):1278-1288
27. Trewyn BG, Slowing II, Giri S, Chen H-T, Lin VSY (2007) Synthesis and Functionalization of a Mesoporous Silica Nanoparticle Based on the Sol-Gel Process and Applications in Controlled Release. Acc Chem Res 40 (9):846-853
28. Trewyn BG, Giri S, Slowing II, Lin VSY (2007) Mesoporous silica nanoparticle based controlled release, drug delivery, and biosensor systems. Chem Commun (31):3236-3245
29. Slowing II, Trewyn BG, Giri S, Lin VSY (2007) Mesoporous silica nanoparticles for drug delivery and biosensing applications. Adv Funct Mater 17 (8):1225-1236
30. Wu S-H, Mou C-Y, Lin H-P (2013) Synthesis of mesoporous silica nanoparticles. Chem Soc Rev 42 (9):3862-3875. doi:10.1039/c3cs35405a
31. Slowing II, Vivero-Escoto JL, Trewyn BG, Lin VSY (2010) Mesoporous silica nanoparticles: structural design and applications. J Mater Chem 20 (37):7924-7937
32. Hoshikawa Y, Yabe H, Nomura A, Yamaki T, Shimojima A, Okubo T (2010) Mesoporous Silica Nanoparticles with Remarkable Stability and Dispersibility for Antireflective Coatings. Chem Mater 22 (1):12-14. doi:10.1021/cm902239a
33. Huh S, Chen H-T, Wiench JW, Pruski M, Lin VSY (2005) Cooperative catalysis by general acid and base bifunctionalized mesoporous silica nanospheres. Angew Chem Int Ed Engl 44 (12):1826-1830
34. Lei J, Wang L, Zhang J (2010) Ratiometric pH sensor based on mesoporous silica nanoparticles and Foerster resonance energy transfer. Chem Commun (Cambridge, U K) 46 (44):8445-8447
35. Mondragon L, Mas N, Ferragud V, de la Torre C, Agostini A, Martinez-Manez R, Sancenon F, Amoros P, Perez-Paya E, Orzaez M (2014) Enzyme- Responsive Intracellular- Controlled Release Using Silica Mesoporous Nanoparticles Capped with e- Poly- l- lysine. Chem Eur J 20 (18):5271-5281. doi:10.1002/chem.201400148
36. Chouikrat R, Seve A, Vanderesse R, Benachour H, Barberi-Heyob M, Richeter S, Raehm L, Durand JO, Verelst M, Frochot C (2012) Non polymeric nanoparticles for photodynamic therapy applications: recent developments. Curr Med Chem 19(6):781–792
37. Couleaud P, Morosini V, Frochot C, Richeter S, Raehm L, Durand JO (2010) Silica-based nanoparticles for photodynamic therapy applications. Nanoscale 2(7):1083–1095. doi:10.1039/c0nr00096e
38. Yamamoto E, Kitahara M, Tsumura T, Kuroda K (2014) Preparation of Size-Controlled Monodisperse Colloidal Mesoporous Silica Nanoparticles and Fabrication of Colloidal Crystals. Chem Mater 26 (9):2927-2933. doi:10.1021/cm500619p
39. Pan L, Liu J, He Q, Wang L, Shi J (2013) Overcoming multidrug resistance of cancer cells by direct intranuclear drug delivery using TAT-conjugated mesoporous silica nanoparticles. Biomaterials 34 (11):2719-2730. doi:10.1016/j.biomaterials.2012.12.040
40. Yi Z, Dumee LF, Garvey CJ, Feng C, She F, Rookes JE, Mudie S, Cahill DM, Kong L (2015) A New Insight into Growth Mechanism and Kinetics of Mesoporous Silica Nanoparticles by in Situ Small Angle X-ray Scattering. Langmuir 31 (30):8478-8487. doi:10.1021/acs.langmuir.5b01637
41. Urata C, Aoyama Y, Tonegawa A, Yamauchi Y, Kuroda K (2009) Dialysis process for the removal of surfactants to form colloidal mesoporous silica nanoparticles. Chem Commun (34):5094-5096. doi:10.1039/b908625k
42. Qiao Z-A, Zhang L, Guo M, Liu Y, Huo Q (2009) Synthesis of Mesoporous Silica Nanoparticles via Controlled Hydrolysis and Condensation of Silicon Alkoxide. Chem Mater 21 (16):3823-3829. doi:10.1021/cm901335k
43. Lu F, Wu SH, Hung Y, Mou CY (2009) Size Effect on Cell Uptake in Well-Suspended, Uniform Mesoporous Silica Nanoparticles. Small 5 (12):1408-1413. doi:10.1002/smll.200900005
44. Ma K, Werner-Zwanziger U, Zwanziger J, Wiesner U (2013) Controlling Growth of Ultrasmall Sub-10 nm Fluorescent Mesoporous Silica Nanoparticles. Chem Mater 25 (5):677-691. doi:10.1021/cm303242h

45. Ma K, Sai H, Wiesner U (2012) Ultrasmall Sub-10 nm Near-Infrared Fluorescent Mesoporous Silica Nanoparticles. J Am Chem Soc 134 (32):13180-13183. doi:10.1021/ja3049783
46. Wu M, Meng Q, Chen Y, Du Y, Zhang L, Li Y, Zhang L, Shi J (2015) Large-pore ultrasmall mesoporous organosilica nanoparticles: Micelle/precursor co-templating assembly and nuclear-targeted gene delivery. Adv Mater (Weinheim, Ger) 27 (2):215-222. doi:10.1002/adma.201404256
47. Pan L, Liu J, He Q, Shi J (2014) MSN-mediated sequential vascular-to-cell nuclear-targeted drug delivery for efficient tumor regression. Adv Mater (Weinheim, Ger) 26 (39):6742-6748. doi:10.1002/adma.201402752
48. Li Z-Y, Liu Y, Hu J-J, Xu Q, Liu L-H, Jia H-Z, Chen W-H, Lei Q, Rong L, Zhang X-Z (2014) Stepwise-acid-active multifunctional mesoporous silica nanoparticles for tumor-specific nucleus-targeted drug delivery. ACS Appl Mater Interfaces 6 (16):14568-14575
49. Pan L, Liu J, Shi J (2014) Intranuclear Photosensitizer Delivery and Photosensitization for Enhanced Photodynamic Therapy with Ultralow Irradiance. Adv Funct Mater 24 (46):7318-7327. doi:10.1002/adfm.201402255
48. Couleaud P, Morosini V, Frochot C, Richeter S, Raehm L, Durand JO (2010) Silica-based nanoparticles for photodynamic therapy applications. Nanoscale 2 (7):1083-1095. doi:10.1039/c0nr00096e
50. Brevet D, Gary-Bobo M, Raehm L, Richeter S, Hocine O, Amro K, Loock B, Couleaud P, Frochot C, Morere A, Maillard P, Garcia M, Durand JO (2009) Mannose-targeted mesoporous silica nanoparticles for photodynamic therapy. Chem Commun (12):1475-1477. doi:10.1039/b900427k
51. Warther D, Jimenez CM, Raehm L, Gerardin C, Durand J-O, Morere A, El Cheikh K, Gallud A, Gary-Bobo M, Maynadier M, Garcia M (2014) Small sized mesoporous silica nanoparticles functionalized with mannose for retinoblastoma cell imaging. RSC Adv 4 (70):37171-37179. doi:10.1039/c4ra05310a
52. Hocine O, Gary-Bobo M, Brevet D, Maynadier M, Fontanel S, Raehm L, Richeter S, Loock B, Couleaud P, Frochot C, Charnay C, Derrien G, Smaihi M, Sahmoune A, Morere A, Maillard P, Garcia M, Durand J-O (2010) Silicalites and Mesoporous Silica Nanoparticles for photodynamic therapy. Int J Pharm 402 (1-2):221-230
53. De Rosa M, Crutchley RJ (2002) Photosensitized singlet oxygen and its applications. Coord Chem Rev 233–234:351–371. doi:10.1016/S0010-8545(02)00034-6